

Recent Lateral Expansion of *Sphagnum* Bogs Over Central Fen Areas of Boreal Aapa Mire Complexes

Lars Granlund,^{1*}  Ville Vesakoski,¹ Antti Sallinen,^{2,3} Tiina H. M. Kolari,¹ Franziska Wolff,² and Teemu Tahvanainen¹

¹Department of Environmental and Biological Sciences, University of Eastern Finland, P.O. Box 111, 80101 Joensuu, Finland;

²Department of Geographical and Historical Studies, University of Eastern Finland, P.O. Box 111, 80101 Joensuu, Finland

³Biodiversity Centre, Finnish Environment Institute SYKE, Lentiirantie 342 B, 88900 Kuhmo, Finland

ABSTRACT

We investigated recent changes in spatial patterning of fen and bog zones in five boreal aapa mire complexes (mixed peatlands with patterned fen and bog parts) in a multiproxy study. Comparison of old (1940–1970s) and new aerial images revealed decrease of flarks (wet hollows) in patterned fens by 33–63% in middle boreal and 16–42% in northern boreal sites, as lawns of bog *Sphagnum* mosses expanded over fens. Peat core transects across transformed areas were used to verify the remote sensing inference with stratigraphic analyses of macrofossils, hyperspectral imaging, and age-depth profiles derived from ¹⁴C AMS dating and pine pollen density. The transect data revealed that

the changes observed by remote sensing during past decades originated already from the end of the Little Ice Age (LIA) between 1700–1850 CE in bog zones and later in the flarks of fen zones. The average lateral expansion rate of bogs over fen zones was 0.77 m y⁻¹ (range 0.19–1.66) as estimated by remote sensing, and 0.71 m y⁻¹ (range 0.13–1.76) based on peat transects. The contemporary plant communities conformed to the macrofossil communities, and distinct vegetation zones were recognized as representing recently changed areas. The fen-bog transition increased the apparent carbon accumulation, but it can potentially threaten fen species and habitats. These observations indicate that rapid lateral bog expansion over aapa mires may be in progress, but more research is needed to reveal if ongoing fen-bog transitions are a commonplace phenomenon in northern mires.

Received 1 July 2021; accepted 3 November 2021;
published online 20 December 2021

Supplementary Information: The online version contains supplementary material available at <https://doi.org/10.1007/s10021-021-00726-5>.

Author contributions TT conceived the research idea and contributed in writing of the entire paper; TT, THMK, LG and VV conducted the field surveys; LG designed and analysed the HSI data and led the writing process of the entire paper; AS conducted the old aerial image analyses including writing on that part; FW conducted UAV image classification including writing on that part; THMK performed the NMDS analysis including writing on that part; VV conducted paleoecology and peat analysis; All authors commented on the manuscript and gave final approval for publication. All authors read and approved the final manuscript

*Corresponding author; e-mail: lars.granlund@uef.fi

Key words: fen-bog transition; peat stratigraphy; soil imaging; hyperspectral imaging; patterned fens; remote sensing; recent peat accumulation; aerial imaging; peatland; vegetation change.

INTRODUCTION

Climate warming is expected to cause a northward shift of vegetation zones (Walther and others 2002). In peatlands, such ecotone movements are conditional to historical legacy of peat formation, hydrology, and vegetation succession. Although predicting future trajectories of peatland development involves great uncertainties, the climatic zonality of peatland types (Parviainen and Luoto 2007; Ruuhijärvi 1960) and predicted movement of climate isoclines gives grounds for the expectation of development of present-day southern peatland formations at more northerly latitudes in the future (Ruosteenoja and others 2011). This expectation is strengthened when it fits recognized trajectories of historical peatland development and connects to known mechanisms of succession. The transition from fen to bog, that is, from shallow-peated minerotrophic mire to thick-peated ombrotrophic peatland, is a well-known successional trajectory connected to climate (Hughes and others 2000; Kuhry and others 1993; Väliiranta and others 2017). Bog growth requires sufficient accumulation of peat and thus, favourable climate to plant production. Indeed, peat accumulation is expected to increase at northern latitudes following lengthening of growing season and increased productivity (Gallego-Sala and others 2018). On the other hand, peat formation is constrained by balance of both primary production and decomposition, and the latter is significantly controlled by hydrology (Górecki and others 2021). Linking impacts of hydrology and climate to peat formation is, however, complicated (Swindles and others 2012) and vegetational changes have important feedback links to mire development. In the fen-bog transition, a major role is played by *Sphagnum* mosses that are the main peat formers of bogs. Increase of *Sphagnum* and shift from fen to bog can increase carbon sequestration (Loisel and Bunsen 2020) and decrease methane emissions (Zhang and others 2021). At the same time, this succession scheme poses additional threat to fen habitats that are already the most endangered habitat types (Janssen and others 2016).

Especially in suboceanic areas, raised bogs represent a southern boreal element, while northern boreal to subarctic zones are characterized by abundance of fens (Parviainen and Luoto 2007; Ruuhijärvi 1960), although both main types occur across the boreal zone in hydrologically distinct parts of peatland complexes. Aapa mires are mixed peatland complexes, where central fen areas are surrounded by marginal bog zones (Laitinen and

others 2007). The proportional cover of fen and bog parts vary in aapa mires; the bog margins getting narrower towards north, while close to the southern fringe of climatic aapa mire zone mire complexes typically have near-equal share of bog and fen vegetation (Tolonen 1967). Most characteristically, the central parts of aapa mires are formed by patterned fens with flarks, that is, wet depressions with quaking moss carpet or open water pools, delineated by hummock strings damming water in flarks and orientated perpendicular to slope. Importantly, aapa mires have concave gross topography with minerotrophic central fen vegetation and shallow peat, and as such they are potential seeds to development of new raised bogs in the future. Although aapa mires are mainly defined in NW Europe, the same definitions (Laitinen and others 2007) apply to most patterned fens in North America as well (Foster and King 1984). Aapa mires can be considered synonymous with patterned fens with the addition that the marginal poor fen and bog areas around patterned fens are accounted in the aapa mire complexes. In contrast, raised bog complexes typically have fen zones in the margins (Howie and Meerveld 2011). The spatial arrangement of bog and fen parts in these mixed peatland complexes are connected to hydrology and topography (Belyea 2007; Laitinen and others 2007) and thus, changing hydrology may change the patterning, indicating added concern to what is expected from changing climate zonation.

Recent studies have found an increase of *Sphagnum* mosses over fen vegetation in pristine aapa mires sensu lato after the Little Ice Age (LIA) and during recent climate change in North America (Loisel and Yu 2013a; Magnan and others 2018; Piilo and others 2019; Primeau and Garneau 2021; Robitaille and others 2021), while few studies have investigated the recent phenomenon in northern Europe (Kolari and others 2021a, b; Väliiranta and others 2017). In Finland, LIA ended approximately 1850 and after the late 1960s the rate of warming has been approximately 0.3 °C per decade (Mikkonen and others 2015). Yet, the effect of climate on fen-bog transition is complicated (Swindles and others 2012; Väliiranta and others 2017), as fen-bog transitions are controlled by several autogenic and allogenic factors. Tahvanainen (2011) demonstrated that similar change can be triggered by disturbance of catchment hydrology: when an aapa mire loses hydrological connection to the upper catchment due to interrupting ditches, bog *Sphagnum* mosses may proliferate to cover flarks within few decades.

Palaeoecological studies of raised bogs have revealed varying timing of bog-fen transition during the Holocene, depending on latitude and elevation (Primeau and Garneau 2021; Väiliranta and others 2017), underlining the case-wise importance of local hydrological conditions (Loisel and Bunsen 2020; Tahvanainen 2011), and of autogenic succession (Piilo and others 2019; Primeau and Garneau 2021).

Most palaeoecological studies of fen-bog transitions have focused on detailed examination of chronology on individual sampling points. However, time series of old aerial images have suggested that changes do not simultaneously encompass the entire mire area (Granlund and others 2021). Instead, *Sphagnum* mosses may expand laterally from margin bogs over central flark fens. Spatial dependence of vegetation transitions has been suggested by some paleoecological studies as well (Loisel and Bunsen 2020; Piilo and others 2019). Aerial photography provides detailed spatial information on vegetation cover and a possibility to investigate recent environmental changes. For example, Dissanska and others (2009) used old aerial images to report a slight increase in open water areas of patterned peatlands in Canada. Yet, remote sensing involves uncertainties, and the imaging can be influenced by seasonal and yearly variation in moisture conditions and vegetation (Dribault and others 2012). Therefore, support by other techniques, such as vegetation sampling (Ihse 2007), is needed for ground-truthing. In contrast, palaeoecological records give finely detailed information on peat layers but commonly have limitations in the number of samples that can be analysed, which makes analysing spatial changes difficult. Hyperspectral imaging (HSI) of peat cores could bridge the gap between these two approaches. Although HSI may lack the precision of detailed palaeoecological analyses, it can be used to effectively process large numbers of samples and to create high resolution maps of peat composition and humification (Granlund and others 2021; Voigt and others 2017), which makes it possible to cover spatial variation of past changes.

In this study, we investigate fen-bog transitions in five pristine boreal aapa mires. More specifically, our focus is on changes in spatial patterning of transition between fen and bog parts of these mixed peatland complexes. We expect peat stratigraphic analyses to confirm recent lateral expansion of bog zones inferred from comparisons of aerial images of different ages and examine if the timing of changes is the same based on the different proxies. We examine if the successional plant

communities inferred by macrofossil analysis of peat profiles conform to modern plant communities across the fen-bog transition zones. We further aim at quantifying the rates of lateral changes and explore with profiles of apparent carbon accumulation rate if the fen-bog transition connects to increase of carbon accumulation. We employ a novel method of hyperspectral imaging of peat cores collected from transects across fen-bog transition zones to enable spatial interpretation of changes. Three of the selected study mires are located in the middle boreal zone, close to the southern limit of aapa mire distribution, and two of the sites are located in the northern boreal zone. We expect that succession from fen to bog is proceeding at an accelerated pace in southern locations and more slowly in the north.

METHODS

Study Sites

The study sites were selected by visually comparing old aerial images (from the mapping unit of Finnish Defence Forces, Topografikunta) with openly available present-day images (National Land Survey of Finland, NLSF). All sites had clear indications of flark area reduction during the last decades, and are characteristic aapa mire complexes located in the main aapa mire climatic region (Ruuhijärvi 1960). Three of the mires (Kalattomansuo, Viitasuo and Ilajansuo) are located in the middle-boreal zone in eastern Finland, where the growing season effective temperature sum (above + 5 °C) has risen from 1070 °C days in 1961–1980 to 1250 °C days in 2001–2020 (Figure 1, ClimGrid data, Finnish Meteorological institute). These sites lie in the Archean bedrock area, mainly formed of granitoids and gneisses. Two sampling sites (Hämeenjäkä East and West) are located in north boreal zone and lie on Proterozoic bedrock area formed of granites. In these more northerly sites, the effective temperature sum has risen from 800 °C days in 1961–1980 to 960 °C days in 2001–2020.

All study sites have grossly similar hydrotopographical patterns and vegetation. Characteristic to aapa mires, central fens have alternating patterning of strings and flarks (Figure 2). Vegetation is characterized by *Menyanthes trifoliata*, *Drosera longifolia*, *Carex limosa*, and *Sphagnum jensenii* in the flark pools, while strings have *Sphagnum angustifolium*, *S. fallax*, *S. papillosum*, *Carex lasiocarpa*, *Eriophorum vaginatum*, and *Trichophorum cespitosum*. The bog zones have patterns of ombrotrophic hummock strings and *Sphagnum* lawns. Hummocks are dom-

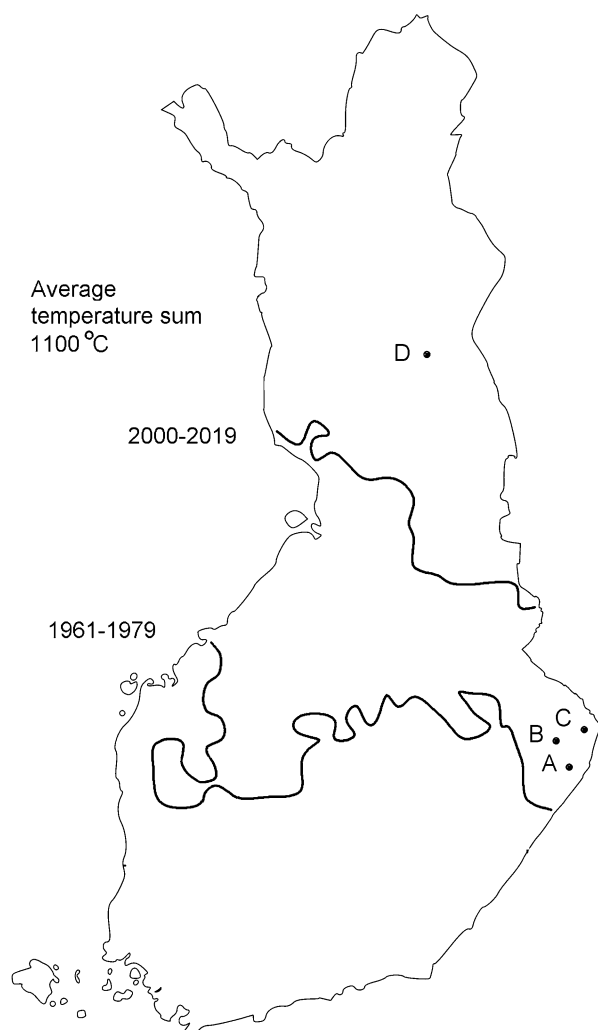


Figure 1. Sampling locations in Finland (a) Kalattomansuo, (b) Viitasuo, (c) Ilajansuo, and (d) Hämeenjätkä East and West. Effective temperature sum of the growing season (1100 °C day isoclines) in 1961–1979 and 2000–2019 (ClimGrid data, Finnish Meteorological institute).

inated by *Sphagnum fuscum* and dwarf-shrubs, such as *Andromeda polifolia* and *Empetrum nigrum*, while *Sphagnum balticum* and *Eriophorum vaginatum* are dominant in lawns.

Flark Change Detection Using Aerial Images

We compared aerial images from different ages to reveal changes in the surface area of flarks. Flark areas were quantified with supervised classifications of the images (Kolari and others 2021b) using ArcGIS 10.7.1. Contemporary (2017–2018) colour infrared aerial images with field resolution of 0.5 m were acquired from the NLSF. Old black and white

aerial images were purchased from the Topografikunta (mapping unit of the Finnish Defense Forces) with differing resolutions and ages: Kalattomansuo 0.86 m, 1944; Viitasuo 0.49 m, 1944; Ilajansuo 0.47 m, 1944; Hämeenjätkä 0.23 m, 1970, respectively. When necessary, low pass filter was applied for reducing the noise present in the old images.

We selected training areas for two classes, flark and non-flark, with ca. one hundred pixels for each class in each mire and time-phase. Maximum likelihood classification was run several times with different training areas, and we selected the areas that best expressed visually interpretable flark boundaries against the bog zones in places where this contrast was most apparent. This was supported by field notes in the cases of new images, while for the old images, no ground validation data was available and thus, the flark classification was more subjective. We converted the classification results to polygon format and corrected minor misclassifications manually, mostly tree shadows or *Sphagnum fuscum* hummocks incorrectly classified as flarks. Afterwards, we assessed the accuracy by inspection of 200–300 random points on each image, of whether the classification as ‘flark’ conformed to location on a visually judged flark pattern or not and calculated the overall accuracies and kappa values. This accuracy estimation does not remove the subjective element of interpretation of the flark patterns but assesses reliability of the maximum likelihood classification. All uncertainties related to old aerial images cannot be removed due to the absence of ground validation, however, a time series from Ilajansuo reveals that these changes had a temporal trend (Supplemental Figure 1).

Classification of Contemporary Hydro-Topographical Patterns

Contemporary images were used to evaluate the current hydro-topographical patterns (ArcGIS Pro 2.7.2) using the aerial images with exception of Kalattomansuo and Viitasuo, from where drone images from 2019 resampled to 0.5 m spatial resolution were used. The images were enhanced by adjusting brightness, contrast, and gamma levels to facilitate classification.

The segmentation tool with ArcGIS pro was used to group neighbouring pixels with similar features into segments. Based on the segmented image, training samples that represented the desired hydro-topographical units ‘‘Wet flark’’, ‘‘String’’, ‘‘Hummock’’, ‘‘Lawn’’, and ‘‘Carpet’’ were designated visually. The training samples were spatially

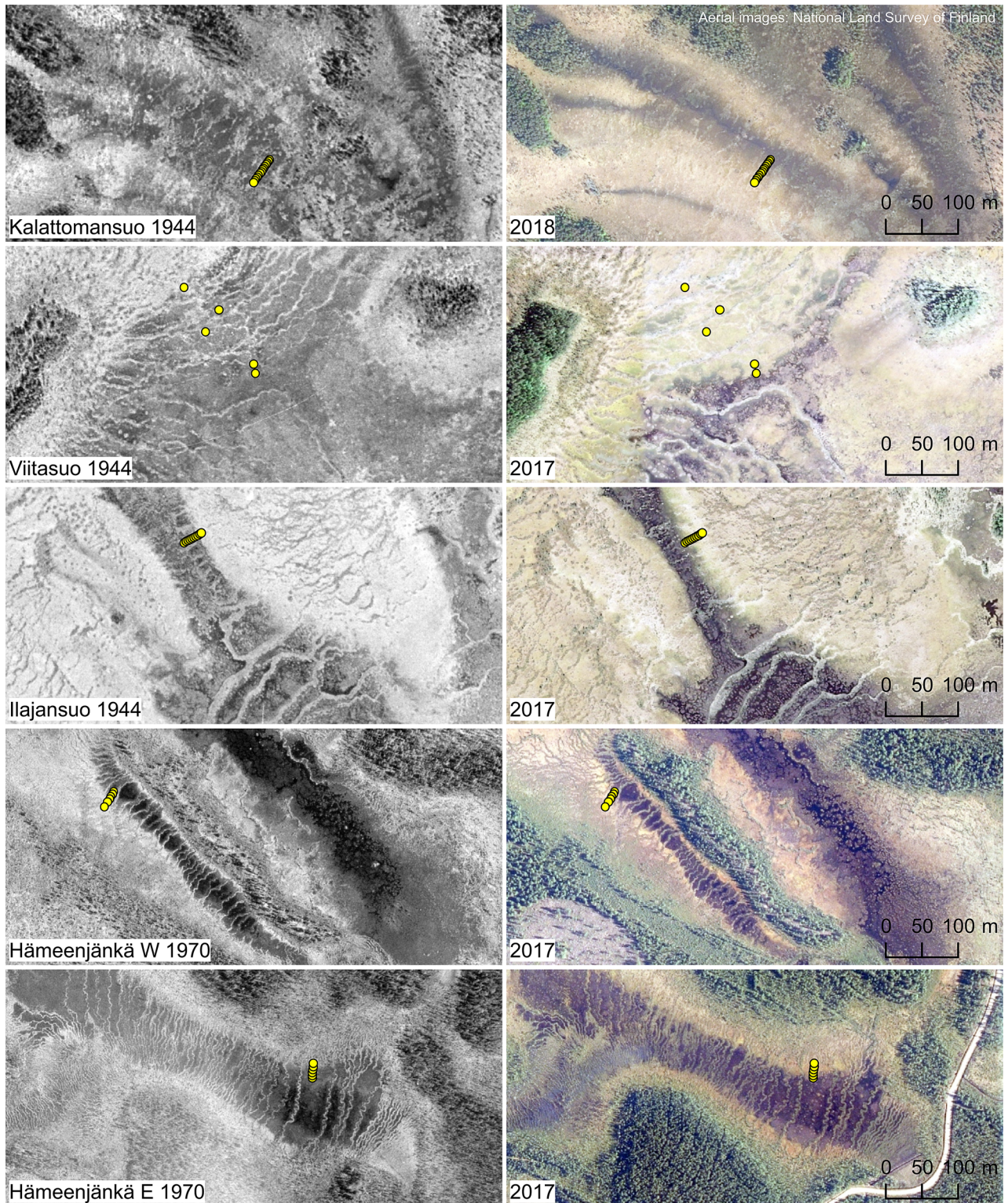


Figure 2. Historical aerial images from the mires selected for sampling (left column) and from 2010's (right column). The peat core sampling transects are indicated with yellow dots. In the aerial images, wet fen flarks are dark, while bog areas and hummock strings dominated by *Sphagnum* mosses appear in pale tones and yellowish color.

distributed across the entire image and the procedure was run for each image separately.

The images were classified with Support Vector Machine (SVM), as it uses a segmented image as input. After the classes were generated, local reclassification of misclassified pixels was done manually. The post-processing also encompassed the filtering of the outcome images to smoothen the respective hydro-topographical classes with low pass filter tool.

Peat and Vegetation Sampling

Altogether 41 peat cores from the five mires were collected during the summer of 2019. Sampling locations were focused on areas between central fen and marginal bog zones, that likely had recent transformations (Figure 2). At each study site, 5–14 peat cores were collected along transects reaching from flark fen to bog zone. All peat cores were collected from between hummock strings. The transects had 3–5-m sampling interval except for the Viitasuo mire, where distances between sampling sites were bigger because of the large area of recent transformation. We refer to the peat cores as being collected from the “flark zone” or the “bog zone” according to the old aerial images. We named the first flark fen sample as ‘0 m’ and the subsequent samples according to their distance from 0 m.

Peat cores were collected with a steel cylinder corer (diameter 12 cm, length 120 cm) specifically crafted for obtaining peat cores with natural shape and unaltered layering, modified from “Clymcorer” (Clymo 1988). The corer has a sharpened edge with a smooth wave, acting as cutting blade, and welded sturdy handles, to aid steady cutting action and lifting. In the sampling procedure, the corer is carefully rotated back-and-forth and slowly descended so that the peat core maintains its natural form and position. When the corer cuts to a desired depth, two steel rods with hooked heads are pushed into the sides of the peat core to help fix it in place. After carefully lifting the corer, the cylinder is pulled while the rods hold the peat profile, and the core is carefully laid on a plastic chute. We cut all peat cores longitudinally in exact halves guided by the plastic chute to reveal undisturbed peat face inside the cores. The cores were wrapped in plastic for transport. In most cases, it was possible to obtain the peat cores in their original length and apparent natural form. However, the samples with the lowest density of buoyant debris and floating moss rafts collected from the flarks were unavoidably compacted, while also in

these cases the cutting action of the corer worked well.

Since our interest lies in recent changes of vegetation, peat cores extended to maximum of 120 cm depth from the surface. Peat depth was measured at all sites with a steel rod. The collected peat cores were kept in + 4 °C for at least 24 h before imaging to ensure they were evenly oxygenated from the surface before the imaging. This was necessary, as changes due to oxidation take place within a few hours after exposure (Granlund and others 2021).

At each peat coring point, we estimated %-cover of all bryophyte and vascular plant species from 0.25 m² vegetation plots and measured water-table depth (WTD) using perforated pipe wells or directly with tape measure in wetter sites. Additional vegetation and water sampling were conducted in 2019 and 2020, comprising 6–12 plots of 3–16 m² and nested subplots (0.25 m²) at each site. At each subplot, pH was measured and a 50-ml water sample was collected. Water samples were analyzed for dissolved organic carbon (DOC) and for calcium concentrations by Inductively Coupled Plasma—Mass Spectrometry).

Hyperspectral Imaging of Peat Cores

We utilized HSI for the detection of peat stratigraphical patterns, based on our earlier experience on peat core imaging (Granlund and others 2021). HSI has been used in mineralogical studies and in soil profile analysis since it can provide both qualitative and quantitative results in high spatial resolution (Hobley and others 2018; Sorenson and others 2020; Stenberg and others 2010). We used HSI to extrapolate information gathered from individual peat cores into a wider data set. We expected that across the study transects, similar peat stratigraphies would be repeated and they could be connected by HSI.

The images were acquired with two hyperspectral cameras by Specim (Spectral Imaging Ltd., Oulu, Finland): the VNIR (visible to near infrared, 400–1000 nm) camera, (ImSpector V10E, FWHM = 3.5 nm) and the SWIR (short-wave infrared, 1000–2500 nm) camera (ImSpector N25E; Specim, FWHM = 12 nm). The samples were illuminated with ten 35 W tungsten halogen lamps, in a 45°/0° geometry. The exposure time was 8.1 ms for VNIR and 2.8 ms for SWIR.

A white spectralon plate used for standardization was included in each image. The average of a minimum of 100 dark current images was subtracted from the sample and white reference ima-

ges. The final reflectance was calculated by dividing the raw sample images with the white reference (Granlund and others 2021). The data correction was done with Fiji (Schindelin and others 2012).

An unsupervised classification method, K-means clustering, was used to detect similarities between the different sampling locations and sites. This approach allows the creation of simplified but comparable maps of peat stratification. The spectral signal is heavily influenced by *Sphagnum* and *Carex* peat and humification, but it may overlook small scale differences in individual peat cores. The classification was run with 8 classes (100 iterations and 10 replications, squared Euclidian distance, Matlab2019b). The analysis included the entire dataset (all mires and samples) and it was calculated for both the VNIR and SWIR datasets. The SWIR data set produced regions that were more consistent with the palaeoecological results (VNIR data not shown).

Palaeoecological Analyses

Three of the peat cores from each site (start, middle, and end of transects) were selected for analysis of plant macrofossil stratigraphies. In addition, main conifer pollen (*Pinus*, *Picea*) and *Sphagnum* spores were counted, as well as occurrence of Cladocera parts that indicate prevalence of aquatic conditions. The sampling locations for peat palaeoecological analyses were selected according to the stratigraphical layers obtained from the K-means clustering analysis of peat core spectral images (Figure 7). We calculated estimates of water-table depth for each peat macrofossil sample, as weighted averages of species weighted averages published by Kolari and others (2021a) using species relative abundances as weights (weighted average calibration) (Ter Braak and Barendregt 1986).

A sample of $20 \pm 3 \text{ cm}^3$, taken from each layer, was simmered in 30 ml 10% potassium hydroxide (10 min, in a sand bed) and after filtration (1 mm mesh filter) marked with Lycopodium spores. 0.5 ml of safranin dye was added to 1 ml of the filtered material. After centrifugation (2000 rpm for 2 min), 0.75 ml of supernatant was removed. All vegetation particles from a 20 μl sample were counted with a microscope (100–400x). The remaining coarse material from the first filtration were counted by examining a 5 cm^2 area on a petri dish with a stereomicroscope (20x). A collection of identified specimens of *Sphagnum* species and tissue samples of the most common vascular plants were used to aid the identification.

Peat Mass and Carbon Accumulation Analyses

Two peat profiles near the opposing ends of the transects were used for dry weight and ash content determinations. The profiles were sampled at 4-cm intervals (4 cm \times 2 cm \times 3 cm) and placed at +55° C for at least 3 days and then weighed. The dried samples were homogenized and subsamples were ignited at 550 °C for at least 3 h and weighed. The apparent carbon accumulation rates (ACAR; $\text{g m}^{-2} \text{ y}^{-1}$) were calculated as peat carbon density divided by the deposition period assuming 50% carbon content of organic material. The recent apparent rate of carbon accumulation (RERCA; $\text{g m}^{-2} \text{ y}^{-1}$) refers to the carbon mass above dated (recent) horizon divided by its age. We estimated RERCA values for the recent period since the end of LIA at ca. 1850 CE. It is important to note that neither ACAR nor RERCA give complete results of true carbon accumulation (Young and others 2021), but they may aid comparisons between sites and studies.

Dating Methods

At each site, we carefully selected and cleansed samples of identified plant material for ^{14}C AMS dating from the ends of the transects. The samples were picked from peat layers connected to changes of peat type based on HSI classification and pollen density profiles. Most samples were leaf or shoot material of vascular plants, while roots were excluded. The samples were washed with distilled water. Altogether 20 samples were used for ^{14}C dating. The ^{14}C analyses were performed by the Poznan Radiocarbon Laboratory (Goslar and others 2004). Calibration was performed using the IntCal04 calibration curve (Reimer and others 2004) and OxCal 4.0 software (Bronk Ramsey 2001).

We prepared continuous profiles of pine pollen density for pollen dating with 2-cm interval of samples (2 cm \times 2 cm \times 2 cm) down to depth of 80 cm. Samples were placed with marker spores in petri dishes with 10% potassium hydroxide (~20 ml). After at least two days (room temperature), the filtered (0.3 mm) pine pollen and marker spores were counted under a microscope (10–40x).

The resulting age curves from pollen deposition were calibrated using the ^{14}C based age determinations. The final age estimation coefficient was determined by approximating the most probable ^{14}C dates. Since pollen calculation has a cumulative error, it was only calculated down to 80 cm and the error was calculated by fitting a coefficient to run

through the external limits of the ^{14}C probability estimations.

Vegetation and Macrofossil Data Analysis

We used non-metric multidimensional scaling (NMDS) to explore and visualize species composition in peat layers recognized by K-means clustering of SWIR hyperspectral data. Plant macrofossil data was combined with vegetation plot data from coring transects and with external vegetation plot data from 23 Finnish aapa mire complexes, including our study sites (T. Kolari, unpublished), to relate palaeoecological records to present-day vegetation. Prior to NMDS analysis, vegetation plot data sets were modified so that they contain information about species, or functional plant groups at the same level as in the plant macrofossil data. As macrofossils were counted in numbers and present-day vegetation was estimated in %-cover, combined data was relativized by plot ($p = 1$). NMDS was performed in PC-ORD 7.04 (McCune and Mefford 2016) using the Sorensen distance measure with a two-dimensional solution, orthogonal principal axes rotation, and randomization test with 249 runs. A spectral index was created from the SWIR data as in Granlund and others (2021), by testing all the possible indices against NMDS axis.

RESULTS

Mire specific results are found in the supplementary file.

Changes of Fen to Bog Zonation

The aerial image analysis of changes in flark area indicated an average loss of 39.0% and range of loss between 16.3% to 62.5% of flark fen area among the studied mire areas (Table 1). At all sites, distinct zones of flark fens still remained, but they were narrowed down remarkably (Figure 2). At one site (Kalattomansuo), flark fen zones were reduced into narrow soaks by appearance of new *Sphagnum*-dominated zones. At other sites the fen-bog zonation persisted, but bog zones advanced from sides over the fen zones (Figure 3).

In most cases, the lost flark areas appeared in modern hydro-topographic patterning as *Sphagnum* carpets (Figure 3). This was most conspicuous in the Ilajansuo mire, where the lost flark areas closely matched with the *Sphagnum* carpet class. In the Viitasuo mire, much of lost flark area indicated by the aerial-image analyses was represented by the drier *Sphagnum* lawn type.

The bog zones had the lowest pH values in all cases, but the differences between the flark and bog zones were small (Table 2). The calcium levels were low and only slightly elevated in two sites. Only one site (Hämeenjäkä West) exhibited the expected pattern with highest pH and calcium and lowest DOC in the flark fen zone, intermediate values in the transition zone and opposing values in the bog zone.

Palaeoecological Analysis of Plant Community Changes

The 8-class K-means clustering revealed a clear general stratigraphic pattern among all analysed peat cores. Three of the classes were characterized by *Sphagnum* peat with differing humification levels (S H1–3, S H2–4, S H4–6) and two classes coincided with mixed peat (CS H3–6, SC H5–7). Three of the classes were estimated to be pure *Carex* peat with differing humification levels (C H4–6, C H6–7, CH7–8) (Figure 4).

The profiles were characterised by a surface layer of pure *Sphagnum* peat with low humification. The only exception was the flark zone sample of Hämeenjäkä East (HE_0m) with mixed CS peat on the surface. In other cases, the top layer was mainly comprised of *Sphagnum* sect. *Cuspidata* (Figure 5) and was generally thicker at the bog end of the sampling transects (Figures 6 and 7). In Ilajansuo, the *Sphagnum* layer was nearly equivalent in depth throughout the transect, but the flark samples were very loose. In a general pattern, the deeper layers were characterised by soft vascular plants, sedge roots and shrub roots and highly humidified peat. The surface and bottom peat layers were separated by layers of mixed peat (SC, CS) with varying depth. In three sites (Ilajansuo, Hämeenjäkä East and Hämeenjäkä West) this three-layer pattern was clearly defined. In two sites (Kalattomansuo and Viitasuo) there were back and forth fluctuations in peat composition with narrow layers of pure *Carex* peat intersecting with *Sphagnum* peat. The reconstructed water-table depth profiles indicated persistence of fairly constant moisture conditions, with the exception of Hämeenjäkä W transition zone profile's higher WTD phase of hummock formation at the transition from *Carex* to *Sphagnum* peat. Cladocera were associated with the deeper layers and *Carex*-peat, and they were nearly absent from the surface layers.

NMDS of combined plant macrofossil and vegetation plot data showed a clear orthogonal pattern of correlations with sampling depth and WTD (Figure 4). The first axis represented the fen-bog

Table 1. Site Descriptive Data, Aerial Image Flark-Area Analysis and Average Water Chemistry results.

	Kalattomansuo	Viitasuo	Ilajansuo	Hämeenjätkä West	Hämeenjätkä East
<i>Site description</i>					
Coordinates	(N) 62°34'12"	62°49'19"	62°55'16"	66°43'3"	66°42'49"
	(E) 30°53'3"	30°37'24"	31°12'40"	27°58'8"	27°59'18"
Elevation above sea level (m)	163	145	172	158	160
Catchment area (ha)	61	76	41	12	27
Catchment drainage (%)	10	3	0	23	10
Open mire area (ha)	38	61	36	6	18
Share of aapa mire flarks (%)	15.5	9.2	10.8	13.7	19.2
Average peat thickness (m)	2.2	2.5	1.8	3.4*	1.9*
Number of peat cores	10	5	6	6	6
<i>Aerial image inference of aapa mire flark area</i>					
Old aerial image year	1944	1944	1944	1970	1970
Old flark area (ha)	8.8	15	6.5	1.4	4.1
Present-day flark area (ha)	5.9	5.6	3.8	0.8	3.4
Change of flark area (%)	– 32.6	– 62.5	– 41.1	– 42.3	– 16.3
Rate of flark change (ha/y)	– 0.039	– 0.129	– 0.037	– 0.013	– 0.015
Accuracy assessment old**	0.93, 0.78	0.89, 0.69	0.95, 0.84	0.95, 0.89	0.95, 0.89
Accuracy assessment new**	0.94, 0.77	0.95, 0.76	0.95, 0.78	0.95, 0.83	0.95, 0.83
<i>Water chemistry (aapa mire flarks—transition zone—bog zone)</i>					
pH	4.1–3.8–3.9	3.8–3.8– 3.6	4.3–3.8– 3.7	4.4–3.9–3.8	3.9–3.7–3.6
Ca (mg/l)	0.4–0.1–0.1	0.1–0.1– 0.1	0.1–0.1– 0.1	0.6–0.5–0.4	0.2–0.2–0.2
DOC (mg/l)	34–26–29	24–27–39	19–17–23	19–38–50	22–27–32
n	4–4–4	4–4–4	4–4–2	2–2–2	2–2–2

*Average peat thickness measured from the sampling sites.

**Accuracy assessment of aerial image classification (overall accuracy, kappa value).

vegetation gradient and the second axis represented variation from wet hollow to hummock vegetation. Deepest peat samples were characterized by vascular plants, mainly *Carex limosa* and *Menyanthes trifoliata*, indicating weak minerotrophy, while peat samples from closer to the surface were most often characterized by *Sphagnum* section Cuspidata. Four peat types derived from K-means clustering had overlapping ranges in the ordination, but little overlap between pure *Sphagnum* peat and pure *Carex* peat. A spectral index $NDI_{1629nm+1705nm}$ had a strong correlation with the first ordination axis (NDI Axis1: Axis 1 $R^2 = 0.59$). No NDI combination had correlation with the Axis 2 (highest $R^2 = 0.10$). The spatial extrapolation of the NMDS ordination scores showed a fine detailed variation in the peat profiles with a shared trend among all profiles of movement from bog to fen vegetation (Figure 4).

Timing of Fen-Bog Transitions and Apparent Carbon Accumulation Profiles

All peat profiles except the Ilajansuo flark fen profile (I_3m) covered the LIA period (ca. 1400–1850 CE) and few profiles covered earlier periods. All age-depth profiles indicated similar patterns with an increasing apparent growth rate associated with transition to *Sphagnum* peat (Figure 6). Since 1850 CE the increment of *Sphagnum* peat growth ranged from 0.71 mm a^{-1} to 3.55 mm a^{-1} . The timing of this transition ranged from 1840–2000 CE in the flark end samples and 1750–1870 CE in the bog end samples.

The peat profiles of the northern site Hämeenjätkä West showed distinct shifts from humified (H 6–7) *Carex* peat with relatively high density ($0.08\text{--}0.15 \text{ g cm}^{-3}$) to weakly humified (H 1–3) *Sphagnum* peat with low density (0.05 g cm^{-3}). The other sites showed similar but less distinct patterns of density and humification. In many profiles

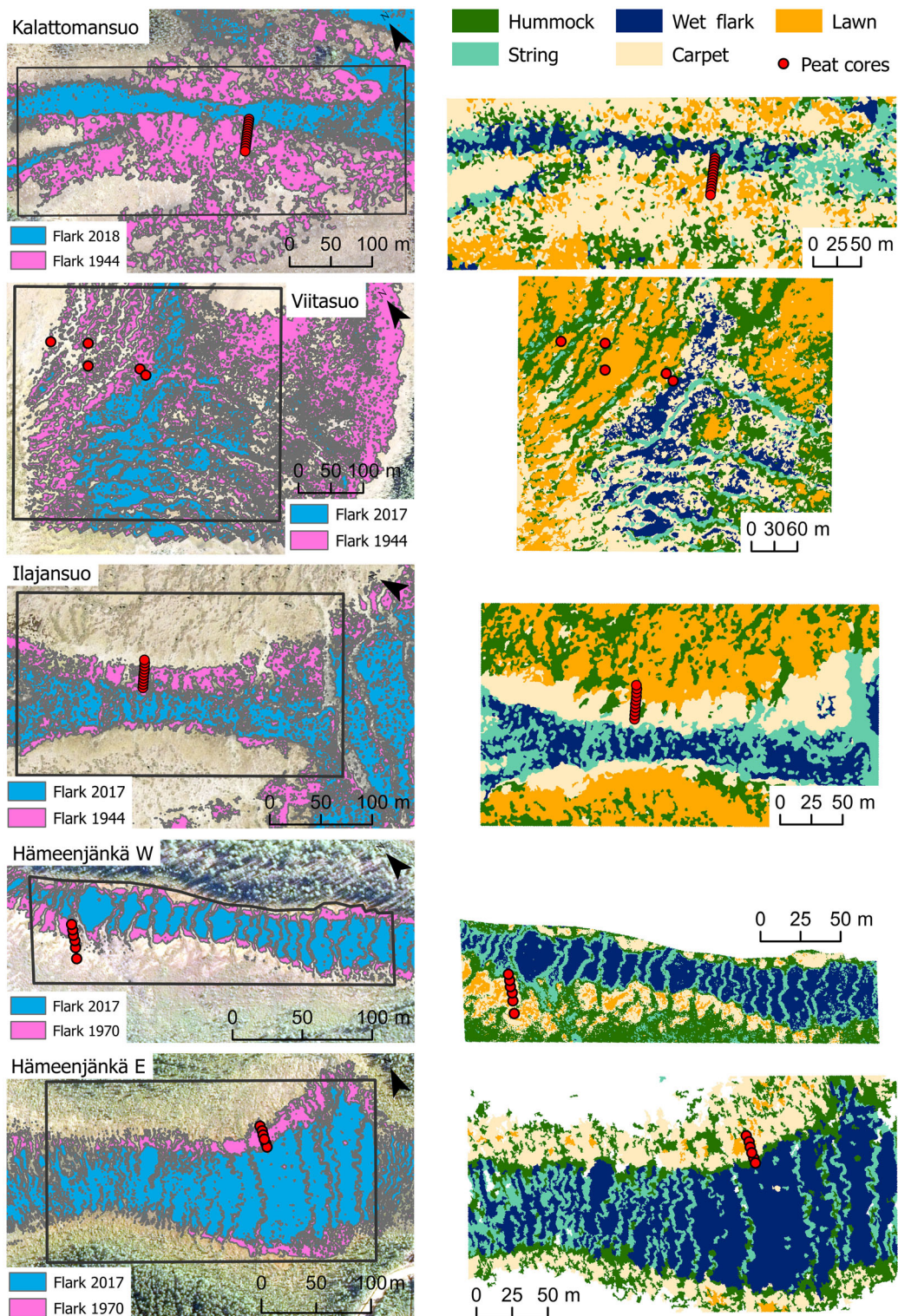


Figure 3. Images of the flark area changes on the left column (pink = transformed area, light blue = current flark area). Classification of contemporary hydro-topographic vegetation patterns on the right column. Sampling locations marked with red dots.

Table 2. Radiocarbon Dating Results, Calibrated Ages and Most Probable Dates According to the Pollen Analysis

Mire	Core	Depth (cm)	Sample	¹⁴ C date	Adjusted dates (CE)	
					Calibrated date	Pollen date**
Ilajansuo	I_3m	43	C. rostrata	122.85 ± 0.35*	1961	1970
		53	C. rostrata	180 ± 30	1770	1920
	I_24m	49	C. rostrata	120 ± 30	1870	1860
		80	Wood	3710 ± 30	-2111	ND
Kalattomansuo	K_0m	28	C. sp	55 ± 30	1866	1890
		39	C. rostrata	160 ± 30	1773	1830
		84	S. palustris	645 ± 30	1369	ND
	K_39m	58	C. sp	260 ± 30	1766	1650
100		C. rostrata	745 ± 30	1256	ND	
Viitasuo	V_12m	36	C. rostrata	106.50 ± 0.33*	1957	1840
		80	C. sp	1510 ± 30	576	560
	V_153m	56	C. rostrata	170 ± 30	1801	1720
		77	E. vaginatum	1310 ± 30	692	780
Hämeenjätkä	HW_4m	36	S. majus	109.73 ± 0.34*	1957	1970
		46	S. Cuspidata sect	120.02 ± 0.36*	1959	1950
		67	C. sp	1970 ± 30	20	ND
		83	Wood	3405 ± 35	-1698	ND
	HW_25m	40	S. papillosum	100 ± 30	1870	1701
		75	Wood	1390 ± 30	638	ND
94	Wood	2880 ± 30	-1052	ND		

*Modern samples pMC/ (ND = not determined).

**Most probable dates from combined ¹⁴C dates and pollen analysis up to 80 cm.

the transition from *Carex* peat or mixed *Carex-Sphagnum* peat to fast-growing *Sphagnum* peat was preceded by clear peaks of ash content. In three cores (I_3m, I_24m, HW_4m) the peak ash content reached over 10% of dry weight.

All profiles had relatively low ACAR during early part of LIA and rise of ACAR towards end of the period (1850 CE) or later, although much variation was revealed between the profiles (Figure 6.). The ACAR values inversely followed changes in density and humification. The RERCA_{1850CE} values in the flark-end samples were 79.3 g C m⁻² y⁻¹, 40.6 g C m⁻² y⁻¹, 74.7 g C m⁻² y⁻¹, and 79.8 g C m⁻² y⁻¹ for Kalattomansuo, Viitasuo, Ilajansuo and Hämeenjätkä West, respectively, and the respective RERCA_{1850CE} values in the bog end were 40.1 g C m⁻² y⁻¹, 35.0 g C m⁻² y⁻¹, 74.3 g C m⁻² y⁻¹ and 19.4 g C m⁻² y⁻¹.

Lateral Expansion Rate of Bog Vegetation

Generally, in the flark fen cores (K_0m, V_12m, I_3m and HW_4m), the transition into *Sphagnum* peat took place later than in the bog zone cores (K_36m, V_153m, I_27m and HW_25m). In Ilajansuo and Hämeenjätkä, the general pattern of flark fen and bog margins persisted despite *Sphag-*

num expansion, whereas in Kalattomansuo and Viitasuo, the general hydrotopographical structure changed more. In Ilajansuo, the mean lateral expansion rate of *Sphagnum* was 0.26 m y⁻¹, as estimated from the aerial images (1944–2019) (Table 3). According to the peat profiles, the transition to *Sphagnum* peat appeared in the bog end sample in 1870 and it took 130 years to appear in the flark end sample of the transect, indicating a transition rate of 0.16 m y⁻¹. In Hämeenjätkä West, the flark retreat took place at a rate of 0.19 m y⁻¹ according to the aerial images (1970–2017), and at the rate of 0.13 m y⁻¹ according to the age profiles (1750, bog end; 1910, flark end). In Kalattomansuo and Viitasuo, the rate of change was higher than in the other sites. In Kalattomansuo the flark retreat took place at a rate of 0.96 m y⁻¹ according to the aerial images (1944–2018) and at the rate of 0.77 m y⁻¹ according to the age profiles (1850, bog end; 1880 flark end). In Viitasuo the flark retreat had at a rate of 1.66 m y⁻¹ in the aerial images (1944–2017) and at the rate of 1.76 m y⁻¹ according to the age profiles (1760, bog end; 1840, flark end).

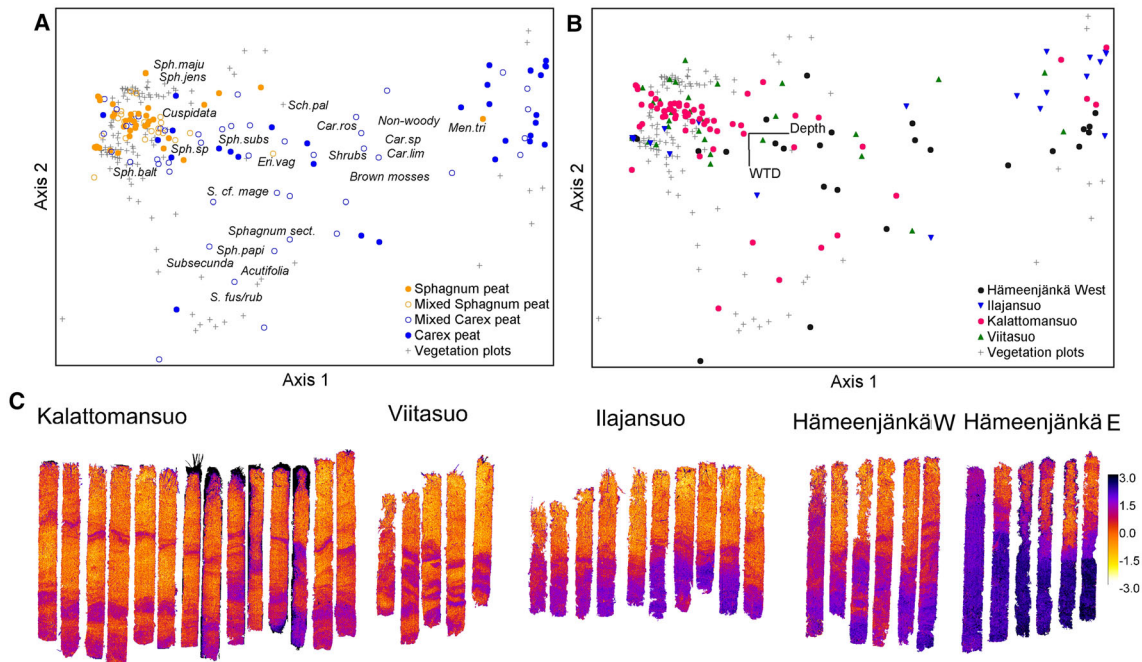


Figure 4. Combined NMDS analysis of the peat core macrofossil samples with vegetation plot data from 23 boreal aapa mires (Tiina Kolari, unpublished data). **a** Peat samples classified in color groups selected from K-means clustering of SWIR hyperspectral data. **b** Peat samples grouped by the sampling mires. The vectors indicate directions of correlations of the depth of peat samples (Depth) and the calibrated water-table depth (WTD). **c** The peat profiles shown with hyperspectral ND index for the NMDS axis 1 ($R^2 = 0.59$). The deep-blue color represents minerotrophic fen vegetation (right in NMDS ordination), and the light-yellow indicates ombrotrophic bog vegetation (left in NMDS ordination).

DISCUSSION

Our palaeoecological investigation proved the lateral expansion of *Sphagnum*-dominated vegetation over the central flark fens in aapa mire complexes observed by remote sensing. The lateral expansion rates of bog vegetation conformed between the remote sensing and peat stratigraphic analyses, but the timing of inferred changes differed remarkably and in the same way at all sites. Indeed, the change from contrasting blackish wet fen surfaces to whitish *Sphagnum* surfaces visible in aerial images was always preceded by change from *Carex* peat to *Sphagnum* peat, dating in most places ca. one hundred years before our oldest aerial images from the 1940's. This indicates that the zone transitions have coincided with post-LIA warming (Luoto and others 2017) and declining precipitation (Helama and others 2009). The contemporary vegetation across the fen-bog ecotones everywhere conformed to peat macrofossil stratigraphies indicating high potential of continuing progress of the phenomenon.

Vegetation Succession and Hydrology

In the fen-bog-transition zone, flark-level species of *Sphagnum* section *Cuspidata* (mainly *S. jensenii* and *S. majus*) had expanded in the central flark fens, forming "quaking" carpets, and same species occurred as first species in transition zones to *Sphagnum* peat in macrofossil stratigraphies. The expanding species are common and frequent in aapa mire flarks and carpets (Laine and others 2009), but they have increased to form continuous carpets in the transition zones of our study sites. Vascular plants were few in the transitional zones, but certain deep-rooted species (*Scheuchzeria palustris*, *Carex limosa*, and *Menyanthes trifoliata* in particular) had persisted through the *Sphagnum* expansion. Present-day vegetation and pH indicated weakly minerotrophic conditions in the flark fens, while calcium concentrations were extremely low in all cases. Weakly minerotrophic fens are sensitive to acidification due to poor mineral buffering and *Sphagnum* mosses can lower pH of their environment (Schweiger and Beierkuhnlein 2017). The results of water chemical analyses indicated an increase of DOC production at some sites, which is likely connected to lower pH in the

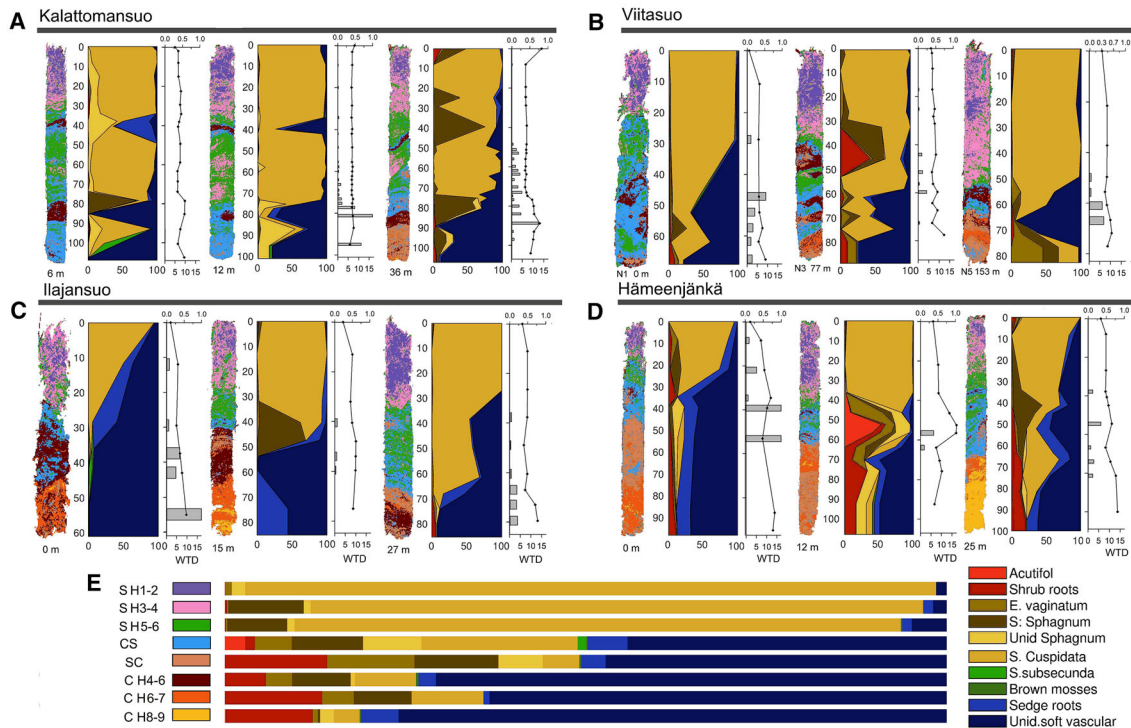


Figure 5. Macrofossil abundance (%) in the Kalattomansuo (a), Viitasuo (b), Ilajansuo (c) and Hämeenjäkä West (d) samples. Distance from the first flark fen sample is indicated under the cores. Plant-species calibrated WTD estimates and relative occurrence of *Cladocera* remains in grey bars. The eight K-means classes from SWIR hyperspectral data (legend on the left) were nominated according to the palaeoecological species estimations (e) (legend on the right).

bog and transition zones compared to the flark fens, as organic acids are chiefly responsible for acidity of mire water in the region (Tahvanainen and others 2002). However, we collected only a limited number of water samples and differences were small, in general.

In the NMDS ordination, the vegetation plot and peat microscopic samples were mixed and formed gradients (1) from ombrotrophic bog communities to minerotrophic fen communities, and (2) from hummock to wet hollow communities. Because much of our sampling transects were represented by homogenous *Sphagnum* carpets and lawns, most of the bog to fen gradient separated the deeper *Carex* peat samples. The bog to fen gradient correlated with an HSI-based index (R^2 0.59) allowing extrapolation of the ordination scores to peat imaging profiles. The resulting image illustrated a general stratification of peat with fen vegetation in deeper layers and bog vegetation near the surface. In two sites (Kalattomansuo and Viitasuo), however, the ordination score imaging indicated finely detailed fluctuation between fen and bog vegetation. The analysis was also successful in combining both plant and peat data, and generally supported the ability of HSI and K-

means clustering in separating *Sphagnum*- and *Carex*-peat (Figure 4a). Peat spectra is influenced by several factors, such as species composition, water content, mineral substances, and peat oxidation. Most importantly, *Carex* and *Sphagnum* peat have different spectral signatures and the spectra are also affected by humification (Granlund and others 2021). However, our results also showed some discrepancies between palaeoecological analysis and HSI in certain locations, probably caused by mixed signals arising from complex peat composition. HSI also provides information only on the exposed face of the peat profile, while microscopy samples reached beneath the peat face (2 cm). One benefit of HSI is the possibility to extrapolate data from point-based measurements (Granlund and others 2021; Steffens and Buddenbaum 2013), and thus we were to increase the number of analysed samples.

Our results indicated a sequence of succession from aquatic sedge fen vegetation to floating rafts of *Sphagnum* (sectio *Cuspidata*), to poor fen lawn vegetation with *S. papillosum* and *Eriophorum vaginatum*, and finally to ombrotrophic bog lawn with *S. balticum*, and sometimes with hummock species, thus, conforming to hydroseral development.

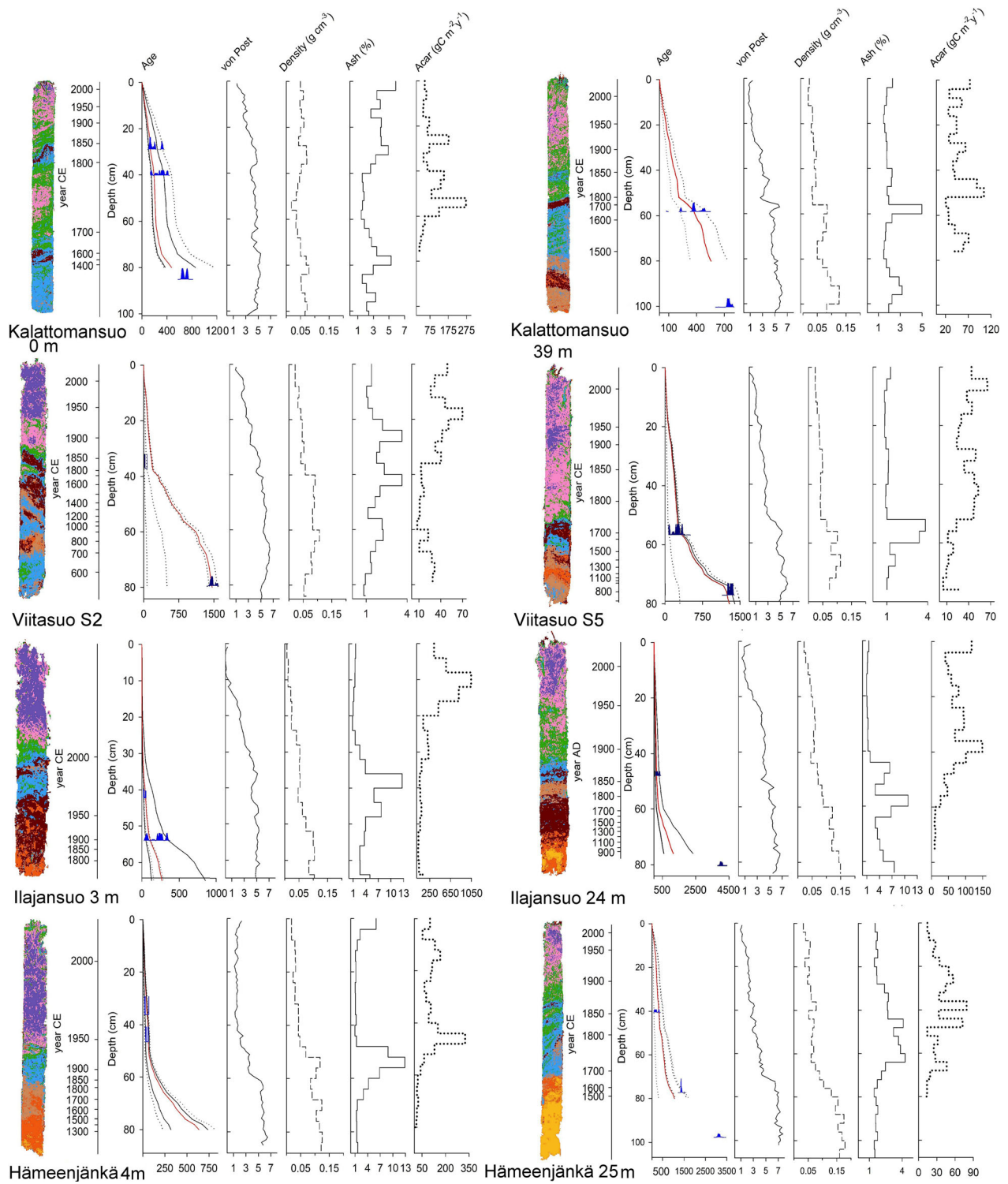


Figure 6. K-means clustering images, age estimations, humification, density, ash and ACAR estimations. The age estimations are based on pollen dating and ^{14}C analysis. The dotted lines indicate the outer limits of ^{14}C calibrations (IntCal04, blue) and the most probable age estimation indicated with red. The von Post estimations are calculated from spectral data $\text{NDVPI}_{\text{NIR}}$.

Elsewhere in Finland, older fen-bog transitions were initiated during dry mid-Holocene climate by

transition from sedge fen to *E. vaginatum* dominated poor fen (Väliranta and others 2017), but

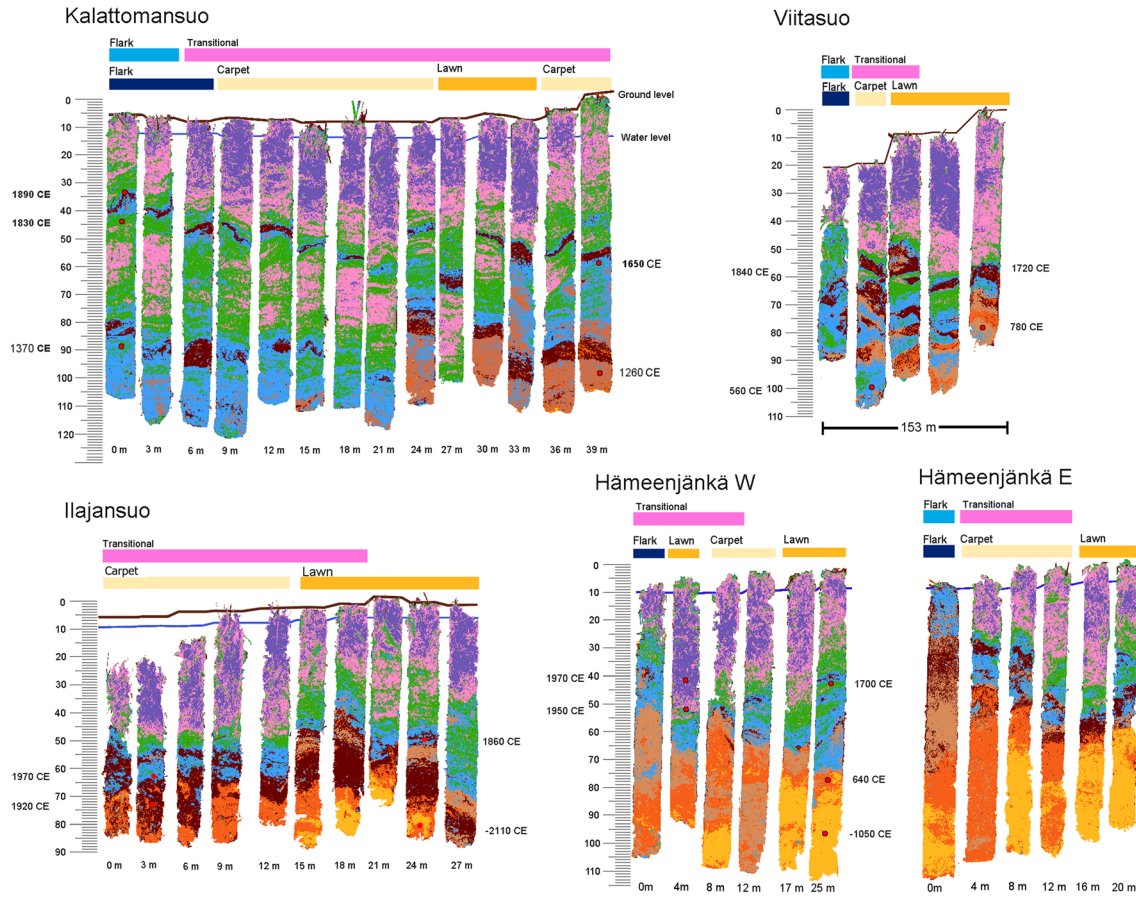


Figure 7. K-means clustering of all the mires in a single analysis (see legend in Figure 5). Brown line = moss surface level. Blue line = water table. The red dots indicate locations for carbon dating and the best age estimate is on the side. The pink and teal horizontal bars indicate the transformed area according to the flark analysis (Figure 3). The lower horizontal bars indicate the modern hydro-topographic classifications (Figure 3).

Table 3. The Onset of *Sphagnum* Expansion and the Flark Retreat in the Sampling Transects.

	Bog expansion from palaeoecological samples				Flark retreat from aerial images		
	Bog end transition (CE)	Flark end transition (CE)	Sample distance (m)	Rate(m y^{-1})	Period	Retreat (m)	Rate(m y^{-1})
Kalattomansuo	1850	1880	39	0.77	1944–2018	71	0.96
Viitasuo	1760	1840	141	1.76	1944–2017	121	1.66
Ilajansuo	1870	2000	21	0.16	1944–2017	19	0.26
Hämeenjätkä W	1750	1910	21	0.13	1970–2017	9	0.19
Hämeenjätkä E	–	–	–	–	1970–2017	14	0.29

without the terrestrialization step by wet *Sphagna*. In eastern Finland, Tolonen (1967) explored many bog profiles and frequently found *E. vaginatum* and

S. magellanicum as transitional vegetation, indicating relatively dry phase during the transition. It is likely that our focus on edges of aapa mire flark

fens brings special character to the successional sequence, while most peat stratigraphic studies of bog-fen transition have focused on single profiles collected from central points of raised bogs. Patterning of aapa mires has secondary origin (Foster and others 1988; Kutenkov and Philippov 2019), and favoured by wet climate phase of the LIA. Thus, the post-LIA situation with open water flarks was different as a starting point of bog succession than mid-Holocene poor fens.

Lateral Expansion of Bogs in Aapa Mire Complexes

The aerial image analysis indicated a very recent and drastic reduction of flark fen area in each study site. There are many uncertainties in the image-based estimation of flark boundaries related to subjectivity of determination, image quality, weather variation, seasonal and yearly fluctuation, and the actual boundaries can be diffuse in nature. In other studies, we have used time-series of fen-to-bog transitions in aapa mires and found that despite variation between individual images these changes had a temporal trend and were not caused by coincidental differences between images (Tahvanainen 2011; Kolari and others 2021b; see also Supplement for time series of the Ilajansuo mire). Kolari and others (2021b) used the same method of flark-identification as in this study, but involving ground validation over a 59-year period in an aapa mire in south-western Finland.

Overall, we recognised two types of change patterns in the mires: (1) a clearly delineated front of *Sphagnum* carpet advanced over fen flarks, while the general zonation between bog and fen parts of the mire remained unchanged (Ilajansuo, Hämeenjäkä East, Hämeenjäkä West), and (2) a patch-wise or diffuse manner of overgrowth of flarks by *Sphagnum* mosses over larger areas (Kalattomansuo and Viitasuo), rather than in clearly advancing fronts. The latter cases had very high lateral expansion rates of *Sphagnum* over wet flark surface, reaching 1.76 m y^{-1} at the Viitasuo mire, as estimated from the transect of peat profiles. At minimum, the Hämeenjäkä W transect indicated a lateral expansion rate of 0.13 m y^{-1} . Remarkably, the remote sensing and peat analyses indicated closely similar rates averaging at 0.77 m y^{-1} and 0.71 m y^{-1} , respectively.

The high rate of lateral expansion of bog vegetation clearly exceeded the rates inferred for raised bogs by paleoecological studies (Korhola 1994; Mäkilä 1997). In part, the high expansion rate is explained by the fact that there are no topographic

obstacles against bog growth over aapa mire flark fens, which are recognized as the main constraint to limit lateral expansion of raised bogs over mineral soil surroundings (Korhola 1994). Similar type of growth has been observed in the infilling of open water karsts (Tsyganov and others 2019) and lentic ecosystems by floating *Sphagnum* mats (Ireland and Booth 2011). In short, central fen flark areas of aapa mire complexes are perhaps the most potential areas for lateral bog growth if conditions favored bog vegetation.

In three sites (Viitasuo, Hämeenjäkä East and Hämeenjäkä West) the *Sphagnum* layer was clearly thicker in the bog end of the sampling transect. In contrast, the thickness of *Sphagnum* peat layer in Ilajansuo varied only a little along the sampling transect. However, thickness does not directly translate into mass, and the samples taken closer to flark fens were not nearly as dense as samples from the bog zones. Peat cores were compacted from the surface after the water was removed. This was visible in all mires, and especially in Ilajansuo the loose *Sphagnum* layer was floating on top of a water column.

Should the spatial advancement of *Sphagnum* continue at the same rate as observed in recent past, the whole flark zones of the studied aapa mires would be covered in about 40 to 230 years. However, it is uncertain whether these aapa mire complexes will achieve a new balance between fen flark and bog areas, or whether they will become true ombrotrophic bogs. In another case study, Tahvanainen (2011) found simultaneous rise of bog vegetation over the whole area of an aapa mire within few decades, caused by dramatic decrease of minerogenic water input due to ditching of the surrounding catchment. Even more rapid proliferation of *Sphagnum* is well documented from mire restoration sites (Haapalehto and others 2014). Indeed, *Sphagnum* carpets have high growth capacity if hydrological conditions changed favorably. In our study sites, hydrological changes were modest compared to drastic impacts of catchment drainage or restoration, but nevertheless, rapid expansion of *Sphagnum*-dominated vegetation was observed.

Timing of Fen-Bog Transitions and Climate

Aerial image analyses indicated increase of *Sphagnum* mosses during the last few decades. Yet, the ^{14}C age estimations revealed that the peat cores had significantly older transitions to the pure *Sphagnum* peat layers on the surface. This demonstrates that

the changes were set on much earlier than observed from aerial images. In each study site, the transition from *Carex*- to *Sphagnum*-peat occurred earlier in the bog end of the sampling transects than in the flark end. This proves that *Sphagnum* bog vegetation started to expand as laterally advancing fronts near the end of LIA. The transition was in progress in the bog end of the study transects in the mid nineteenth century in Viitasuo and Hämeenjätkä. The transects spanned 80 years of bog expansion in Viitasuo and 160 years in Hämeenjätkä. Despite the lack of exact synchronicity between the samples, the oldest signs of bog expansion were always dated near the end of LIA. As the studied case of fen-bog transition represents a laterally advancing *Sphagnum* front, estimating the precise timing of fen-bog transition from individual peat cores is rather arbitrary, which has been considered also in other studies (Lamarre and others 2012; Piilo and others 2019).

The peat age estimates were constructed from ^{14}C dating amended with cumulative pine pollen density calculations. Dating based on pine pollen is inherently somewhat inaccurate, as pollen deposition fluctuates through time and errors are cumulative. We tested for a correction of pollen calculation using estimated historical fluctuation data of pollen deposition in the study region (Pitkänen and Huttunen 1999), however, the effects were negligible (data not shown). Linking these results with ^{14}C dating allowed the estimation of dates for the fen-bog transitions. Overall, the ^{14}C dates corresponded to the pollen estimates. Yet the ^{14}C age estimates from Viitasuo (V_12m) had poor accordance with pollen estimate, and the Hämeenjätkä West ^{14}C age estimates below 50 cm were older than expected by the pollen analysis. It is probable that the analysed wood samples from Hämeenjätkä represented older material than the peat strata they were collected from. Individual ^{14}C age estimates from fen peat can also be unreliable (Väliranta and others 2014).

In our study sites, the earliest signs of *Sphagnum* expansion occurred near the end of the LIA (~ 1750–1870 CE). Indeed, warmer climatic conditions and longer growing season favour *Sphagnum* growth (Bengtsson and others 2021; Gallego-Sala and others 2018) if moisture supply is not limited (Loisel and others 2012). Post-LIA climate development likely involved complex seasonal changes besides average temperatures and precipitation, affecting duration of seasonal frost and snow-melt discharge patterns, complicating the interpretation of causes of fen-bog change. Furthermore, two of our study transects, peat strati-

ographies indicated back and forth transformations between fen and bog vegetation before the recent trend. Aapa mires and patterned fens are susceptible to climatic forcing due to prospects of climate change in northern latitudes of their distribution. Yet, pure climatic forcing is an overly simplistic view and both allogenic and autogenic factors can drive succession (Swindles and others 2012; Kolari and others 2021b).

Although there was a discrepancy regarding the time of onset of *Sphagnum* expansion according to our dated peat profiles and aerial image-based age estimation, the rate of change was nearly identical according to both methods. Our results suggest that the fen-bog transition has taken place in phases: first as loose infilling of open-water pools and in the second phase, *Sphagnum* mosses forming thicker, continuous carpets and water-table depth increasing with the progressive growth. It is not until the latter phase, when changes become visible in aerial images. This gives an important caveat on overinterpretation of remote sensing of changes and underlines the need for multiple proxies, such as peat stratigraphic examination to support interpretation.

Effects on Apparent Carbon Accumulation

The future of carbon accumulation in northern peatlands is uncertain (Loisel and others 2021). Extensive lowering of water table and subsequent increase of decomposition rates may turn peatlands from carbon sinks to carbon sources (Swindles and others 2019). Yet, *Sphagnum*-dominated bogs tend to have higher carbon accumulation than fens (Loisel and Bunsen 2020), and the fen-bog transition often coincides with a drastic increase in carbon accumulation rates (Loisel and Yu 2013a; Loisel and Yu 2013b). Indeed, recent studies of fen-bog transitions have found substantial increases of peat accumulation (Piilo and others 2019; Primeau and Garneau 2021). However, estimating recent changes of carbon accumulation is fundamentally unreliable; higher apparent accumulation rates (ACAR, RERCA) are expected in the surface peat only due to incomplete decomposition and interpretation of apparent accumulation profiles does not infer true accumulation of the time periods concerned (Loisel and Bunsen 2020; Young and others 2021). However, steep changes of ACAR curves, when connected with changes of peat forming vegetation, can indicate connected changes of carbon cycle, if not quantification, and RE-

RCA values give chance for robust comparisons between sites (Loisel and Bunsen 2020).

Northern peatlands with recent fen-bog transitions have recorded RERCA_{1850CE} values between 53 and 140 g C m⁻² y⁻¹ (Lamarre and others 2012; Primeau and Garneau 2021; Robitaille and others 2021). These values have increased during recent years (RERCA_{1950CE}). We recorded slightly lower RERCA_{1850CE} values in the fen flark zone: 79.3, 40.6, 74.7, and 79.8 g C m⁻² y⁻¹ for Kalattoman-suo, Viitasuo, Ilajansuo and Hämeenjätkä West, respectively. The respective RERCA_{1850CE} values in the bog end were lower in all cases: 40.1, 35.0, 74.3, and 19.4 g C m⁻² y⁻¹. This indicates that the early phase of fen-bog transition has high carbon accumulation rate that slows down as the process advances. It is notable that only in Ilajansuo the flark end sample did not show higher RERCA than the bog sample. However, the increase of *Sphagnum* took place only very recently (ca. 2000 CE) in the flark end of Ilajansuo sampling transect, and therefore the change was not yet realised in the post-LIA RERCA estimate.

We found sudden steep transitions in ACAR values that reflected the change from *Carex* peat to *Sphagnum* peat. In many cases the high ACAR values were preceded by high peaks in ash content. This phenomenon of high ash content has been recorded in unison, or adjacent to fen-bog transitions (Granlund and others 2021; Kokfelt and others 2009). Atmospheric mineral deposition of dust particles or changing peat decomposition rates can cause high peaks in ash content (Ferrat and others 2012). However, these peaks could be due to the accumulation of biogenic silica caused by the increase of diatoms in transitional ecosystems (Kokfelt and others 2009; Tahvanainen 2011).

In general, our results indicated an increase in carbon accumulation related to fen-bog transitions. Increased carbon accumulation in both fens and bogs is expected due to increasing growing degree days above 0 °C (GDD0) and cumulative photosynthetically active radiation during the growing season (PAR0) (Charman and others 2013; Gallego-Sala and others 2018). Fens are sensitive towards climate-driven increase in carbon accumulation and rapid transitions in vegetation can have further impact on carbon accumulation. Yet, after the initial burst of rapid growth, the accumulation rate seems to slow down. The bog expansion over fen vegetation may also reduce CH₄ emissions (Zhang and others 2021), which is highly important, since fens can have more than three times as high emissions than bog vegetation (Treat and others 2018).

CONCLUSIONS

This study combined multiproxy data of aerial images, palaeoecological peat analyses, hyperspectral imaging, plant macrofossils, dating, and modern vegetation data to investigate recent fen-bog transitions in aapa mire complexes. The aerial images revealed drastic reduction in flark fen areas during the twentieth century and these were confirmed with peat core transects. The onset of the observed fen-bog transitions was earlier than estimated from the aerial images. In each study site, the *Sphagnum* increase had begun near the end of the LIA (~ 1850 CE) but had only become visible in aerial images during the twentieth century. At two mire areas, *Sphagnum*-dominated bog vegetation zones had expanded over flark areas as spatially explicit fronts, while in two cases the change was more diffuse. The plant macrofossil records corresponded to the spatial patterns of present-day vegetation, indicating potentially ongoing and laterally expanding fen-bog transition in our study sites.

The transition from flark fen to *Sphagnum*-dominated bogs involved an increase in apparent carbon accumulation; however, the rate of carbon accumulation was found to slow down as the fen-bog transition proceeded. Although the increase of *Sphagnum*-dominated bog vegetation would likely translate to increased carbon sink capacity and decreased methane emissions of northern aapa mires, the fen-bog succession scheme has two sides. Fens have high biodiversity and provide habitats for many specialized species, and among the mire habitat types, fens are the most threatened. Therefore, rapidly proceeding *Sphagnum* expansion can potentially threaten mire species and habitats.

ACKNOWLEDGEMENTS

We would like to thank Julie Loisel and Paul Morris for valuable comments on the manuscript. Pasi Korpelainen and Timo Kumpula provided helpful advice in remote sensing analyses. We also thank Laura Koivu, Maiju Tanskanen and Sauli Mäkinen for assistance in the laboratory. Markku Keinänen and Sarita Keski-Saari gave valuable comments on the manuscript. Funding was provided by Academy of Finland (SHIFTMIRE, decision 311655), Jenny and Antti Wihuri foundation (LG), the Finnish Cultural Foundation (THMK), and the Kone Foundation (AS; FW). The research was partially supported by the Academy of Finland Flagship Programme, Photonics Research and Innovation

(PREIN, decision 320166) and the Finnish National Plant Phenotyping Infrastructure (NaPPI).

FUNDING

Open access funding provided by University of Eastern Finland (UEF) including Kuopio University Hospital.

OPEN ACCESS

This article is licensed under a Creative Commons Attribution 4.0 International License, which permits use, sharing, adaptation, distribution and reproduction in any medium or format, as long as you give appropriate credit to the original author(s) and the source, provide a link to the Creative Commons licence, and indicate if changes were made. The images or other third party material in this article are included in the article's Creative Commons licence, unless indicated otherwise in a credit line to the material. If material is not included in the article's Creative Commons licence and your intended use is not permitted by statutory regulation or exceeds the permitted use, you will need to obtain permission directly from the copyright holder. To view a copy of this licence, visit <http://creativecommons.org/licenses/by/4.0/>.

REFERENCES

- Belyea LR. 2007. Climatic and topographic limits to the abundance of bog pools. *Hydrol Process* 21(5):675–687. <https://doi.org/10.1002/hyp.6275>.
- Bengtsson F, Rydin H, Baltzer JL, Bragazza L, Bu Z, Caporn SJM, Dorrepaal E, Flatberg KI, Galanina O, Gałka M, and others 2021. Environmental drivers of sphagnum growth in peatlands across the holarctic region. *J Ecol* 109(1):417–431. <https://doi.org/10.1111/1365-2745.13499>
- Bronk Ramsey C. 2001. Development of the radiocarbon calibration program. *Radiocarbon* 43(2A):355–363. <https://doi.org/10.1017/S0033822200038212>.
- Charman DJ, Beilman DW, Blaauw M, Booth RK, Brewer S, Chambers FM, Christen JA, Gallego-Sala A, Harrison SP, Hughes PDM, and others 2013. Climate-related changes in peatland carbon accumulation during the last millennium. *Biogeosciences* 10(2):929–944. <https://doi.org/10.5194/bg-10-929-2013>.
- Clymo RS. 1988. A high-resolution sampler of surface peat. *Functional Ecology* 2:425–431.
- Dissanska M, Bernier M, Payette S. 2009. Object-based classification of very high resolution panchromatic images for evaluating recent change in the structure of patterned peatlands, *Canad J Remote Sens* 35(2):189–215. <https://doi.org/10.5589/m09-002>.
- Dribault Y, Chokmani K, Bernier M. 2012. Monitoring seasonal hydrological dynamics of minerotrophic peatlands using multi-date GeoEye-1 very high resolution imagery and object-based classification. *Remote Sens* 4(7):1887–1912. <https://doi.org/10.3390/rs4071887>.
- Ferrat M, Weiss DJ, Spiro B, Large D. 2012. The inorganic geochemistry of a peat deposit on the eastern qinghai-tibetan plateau and insights into changing atmospheric circulation in central asia during the holocene. *Geochim Cosmochim Acta* 91:7–31. <https://doi.org/10.1016/j.gca.2012.05.028>.
- Foster DR, King GA. 1984. Landscape features, vegetation and developmental history of a patterned fen in south-eastern labrador, canada. *J Ecol* 72(1):115–143. <https://doi.org/10.2307/2260009>.
- Foster DR, King GA, Santelmann MV. 1988. Patterned fens of western labrador and adjacent quebec: Phytosociology, water chemistry, landform features, and dynamics of surface patterns. *Can J Bot* 66(12):2402–2418. <https://doi.org/10.1139/b88-327>.
- Gallego-Sala A, Charman DJ, Brewer S, Page SE, Prentice IC, Friedlingstein P, Moreton S, Amesbury MJ, Beilman DW, Björck S, and others 2018. Latitudinal limits to the predicted increase of the peatland carbon sink with warming. *Nature Climate Change* 8(10):907–913. <https://doi.org/10.1038/s41558-018-0271-1>
- Górecki K, Rastogi A, Stróżecki M, Gałka M, Lamentowicz M, Luców D, Kayzer D, Juszczak R. 2021. Water table depth, experimental warming, and reduced precipitation impact on litter decomposition in a temperate sphagnum-peatland. *Science Total Environment* 771:145452. <https://doi.org/10.1016/j.scitotenv.2021.145452>.
- Goslar T, Czernik J, Goslar E. 2004. Low-energy 14C AMS in poznań radiocarbon laboratory, poland. *Nucl Instrum Meth B* 223–224:5–11. <https://doi.org/10.1016/j.nimb.2004.04.005>.
- Granlund L, Keinänen M, Tahvanainen T. 2021. Identification of peat type and humification by laboratory VNIR/SWIR hyperspectral imaging of peat profiles with focus on fen-bog transition in aapa mires. *Plant Soil* 460(1):667–686. <https://doi.org/10.1038/s41558-018-0271-1>.
- Haapalehto T, Kotiaho JS, Matilainen R, Tahvanainen T. 2014. The effects of long-term drainage and subsequent restoration on water table level and pore water chemistry in boreal peatlands. *J Hydrol* 519:1493–1505. <https://doi.org/10.1016/j.jhydrol.2014.09.013>.
- Helama S, Merilainen J, Tuomenvirta H. 2009. Multicentennial megadrought in northern Europe coincided with a global El Niño-Southern Oscillation drought pattern during Medieval Climate Anomaly. *Geology*. 37:175–178. <https://doi.org/10.1130/G25329A.1>.
- Hobley E, Steffens M, Bauke SL, Kögel-Knabner I. 2018. Hot-spots of soil organic carbon storage revealed by laboratory hyperspectral imaging. *Sci Rep* 8(1):13900. <https://doi.org/10.1038/s41598-018-31776-w>.
- Howie SA, Meerveld IT. 2011. The essential role of the lag in raised bog function and restoration: A review. *Wetlands* 31(3):613–622. <https://doi.org/10.1007/s13157-011-0168-5>.
- Hughes PDM, Mauquoy D, Barber KE, Langdon PG. 2000. Mire-development pathways and palaeoclimatic records from a full holocene peat archive at walton moss, cumbria, england. *The Holocene* 10(4):465–479. <https://doi.org/10.1191/095968300675142023>.
- Ihse M. 2007. Colour infrared aerial photography as a tool for vegetation mapping and change detection in environmental studies of nordic ecosystems: A review. *Nor Geogr Tidsskr* 61(4):170–191. <https://doi.org/10.1080/00291950701709317>.

- Ireland AW, Booth RK. 2011. Hydroclimatic variability drives episodic expansion of a floating peat mat in a north american kettlehole basin. *Ecology* 92(1):11–18. <https://doi.org/10.1890/10-0770.1>.
- Janssen JAM, Janssen JAM, Rodwell JS, Garcia Criado M, Gubbay S, Haynes T, Nieto A, Sanders N, Landucci F, Loidi J, and others. 2016. European red list of habitats - part 2. terrestrial and freshwater habitats. <https://doi.org/10.2779/091372>
- Kokfelt U, Struyf E, Randsalu L. 2009. Diatoms in peat – dominant producers in a changing environment? *Soil Biology and Biochemistry* 41(8):1764–1766. <https://doi.org/10.1016/j.soilbio.2009.05.012>.
- Kolari THM, Korpelainen P, Kumpula T, Tahvanainen T. 2021a. Accelerated vegetation succession but no hydrological change in a boreal fen during 20 years of recent climate change. *Ecol Evol* 11:7602–7621. <https://doi.org/10.1002/ece3.7592>
- Kolari TH, Sallinen A, Wolff F, Kumpula T, Tolonen K, Tahvanainen T. 2021b. Ongoing fen–bog transition in a boreal aapa mire inferred from repeated field sampling, aerial images, and landsat data. *Ecosystems*. <https://doi.org/10.1007/s10021-021-00708-7>
- Korhola AA. 1994. Radiocarbon evidence for rates of lateral expansion in raised mires in southern finland. *Quatern Res* 42(3):299–307. <https://doi.org/10.1006/qres.1994.1080>.
- Kuhry P, Nicholson BJ, Gignac LD, Vitt DH, Bayley SE. 1993. Development of sphagnum-dominated peatlands in boreal continental canada. *Can J Bot* 71(1):10–22. <https://doi.org/10.1139/b93-002>.
- Kutenkov SA, Philippov DA. 2019. Aapa mire on the southern limit: A case study in vologda region (north-western russia). *Mires and Peat* 24(10):1–20. <https://doi.org/10.19189/MaP.2018.OMB.355>.
- Laine J, Harju P, Timonen T, Laine A, Tuittila E, Minkkinen K, Vasander H. 2009. The intricate beauty of sphagnum mosses. Helsinki: University of Helsinki Department of Forest Ecology.
- Laitinen J, Rehell S, Huttunen A, Tahvanainen T, Heikkilä R, Lindholm T. 2007. Mire systems in finland - special view to aapamires and their water-flow pattern. 58(1):1,1–26.
- Lamarre A, Garneau M, Asnong H. 2012. Holocene paleohydrological reconstruction and carbon accumulation of a permafrost peatland using testate amoeba and macrofossil analyses, kuujuarapik, subarctic québec, canada. *Rev Palaeobot Palynol* 186:131–141. <https://doi.org/10.1016/j.revpa.2012.04.009>
- Loisel J, Gallego-Sala A, Yu Z. 2012. Global-scale pattern of peatland *sphagnum* growth driven by photosynthetically active radiation and growing season length. *Biogeosciences* 9(7):2737–2746. <https://doi.org/10.5194/bg-9-2737-2012>
- Loisel J, Gallego-Sala A, Amesbury MJ, Magnan G, Anshari G, Beilman DW, Benavides JC, Blewett J, Camill P, Charman DJ, and others 2021. Expert assessment of future vulnerability of the global peatland carbon sink. *Nature Climate Change* 11(1):70–77. <https://doi.org/10.1038/s41558-020-00944-0>
- Loisel J, Bunsen M. 2020. Abrupt fen-bog transition across southern patagonia: Timing, causes, and impacts on carbon sequestration. *Front Ecol Evol* 8:273. <https://doi.org/10.3389/fevo.2020.00273>
- Loisel J, Yu Z. 2013a. Recent acceleration of carbon accumulation in a boreal peatland, south central alaska. *J Geophys Res Biogeosci* 118(1):41–53. <https://doi.org/10.1029/2012JG001978>.
- Loisel J, Yu Z. 2013b. Surface vegetation patterning controls carbon accumulation in peatlands. *Geophys Res Lett* 40(20):5508–5513. <https://doi.org/10.1002/grl.50744>.
- Luoto T, Kivilä E, Rantala M, Nevalainen L. 2017. Characterization of the Medieval Climate Anomaly, Little Ice Age and recent warming in northern Lapland. *Int. J. Climatol* 37:1257–1266. <https://doi.org/10.1002/joc.5081>.
- Magnan G, van Bellen S, Davies L, Froese D, Garneau M, Mullan-Boudreau G, Zaccone C, Shotyck W. 2018. Impact of the little ice age cooling and 20th century climate change on peatland vegetation dynamics in central and northern alberta using a multi-proxy approach and high-resolution peat chronologies. *Quat Sci Rev* 185:230–243. <https://doi.org/10.1016/j.quascirev.2018.01.015>.
- Mäkälä M. 1997. Holocene lateral expansion, peat growth and carbon accumulation on haukkasuo, a raised bog in south-eastern finland. *Boreas* 26(1):1–14. <https://doi.org/10.1111/j.1502-3885.1997.tb00647.x>.
- McCune B and Mefford MJ. 2016. PC-ORD. multivariate analysis of ecological data. version 7.0 for windows.
- Mikkonen S, Laine M, Mäkelä HM, Gregow H, Tuomenvirta H, Lahtinen M, Laaksonen A. 2015. Trends in the average temperature in finland, 1847–2013. *Stochastic Environmental Research and Risk Assessment* 29(6):1521–1529. <https://doi.org/10.1007/s00477-014-0992-2>.
- Parviainen M, Luoto M. 2007. Climate envelopes of mire complex types in fennoscandia. *Geogr Ann A* 89(2):137–151. <https://doi.org/10.1111/j.1468-0459.2007.00314.x>.
- Piilo S.R., Zhang H, Garneau M, Gallego-Sala A, Amesbury MJ, Väiliranta MM. 2019. Recent peat and carbon accumulation following the little ice age in northwestern québec, canada. *Environ Res Lett* 14(7):075002. <https://doi.org/10.1088/1748-9326/ab11ec>.
- Pitkänen A, Huttunen P. 1999. A 1300-year forest-fire history at a site in eastern finland based on charcoal and pollen records in laminated lake sediment. *The Holocene* 9(3):311–320. <https://doi.org/10.1191/095968399667329540>.
- Primeau G and Garneau M. 2021. Carbon accumulation in peatlands along a boreal to subarctic transect in eastern canada. *The Holocene* 31(5):858–869. <https://doi.org/10.1177/0959683620988031>.
- Reimer PJ, Baillie MGL, Bard E, Bayliss A, Beck JW, Bertrand CJH, Blackwell PG, Buck CE, Burr GS, Cutler KB, and others 2004. IntCal04 terrestrial radiocarbon age calibration, 0–26 cal kyr BP. *Radiocarbon* 46(3):1029–1058.
- Robitaille M, Garneau M, van Bellen S, Sanderson NK. 2021. Long-term and recent ecohydrological dynamics of patterned peatlands in north-central quebec (canada). *The Holocene* 31(5):844–857. <https://doi.org/10.1177/0959683620988051>.
- Ruosteenoja K, Räisänen J, Pirinen P. 2011. Projected changes in thermal seasons and the growing season in finland. *Int J Climatol* 31(10):1473–1487. <https://doi.org/10.1002/joc.2171>.
- Ruuhijärvi R. 1960. Über die regionale einteilung der nordfinnischen moore. *Annales Botanici Societatis Zoologici Botanici Fennicae 'vanamo'* 31(1):1–360.
- Schindelin J, Arganda-Carreras I, Frise E, Kaynig V, Longair M, Pietzsch T, Preibisch S, Rueden C, Saalfeld S, Schmid B, and others 2012. Fiji: An open-source platform for biological-image analysis. *Nat Meth* 9(7):676–682. <https://doi.org/10.1038/nmeth.2019>.
- Schweiger AH, Beierkuhnlein C. 2017. The ecological legacy of 20th century acidification carried on by ecosystem engineers.

- Appl Veg Sci 20(2):215–224. <https://doi.org/10.1111/avsc.12259>.
- Sorenson PT, Quideau SA, Rivard B, Dyck M. 2020. Distribution mapping of soil profile carbon and nitrogen with laboratory imaging spectroscopy. *Geoderma* 359:113982. <https://doi.org/10.1016/j.geoderma.2019.113982>.
- Steffens M, Buddenbaum H. 2013. Laboratory imaging spectroscopy of a stagnic luvisol profile—high resolution soil characterisation, classification and mapping of elemental concentrations. *Geoderma* 195–196:122–132. <https://doi.org/10.1016/j.geoderma.2012.11.011>.
- Stenberg B, Viscarra Rossel RA, Mouazen AM, Wetterlind J. 2010. Chapter five - visible and near infrared spectroscopy in soil science. *Advances in Agronomy* 107:163–215. [https://doi.org/10.1016/S0065-2113\(10\)07005-7](https://doi.org/10.1016/S0065-2113(10)07005-7).
- Swindles GT, Morris PJ, Baird AJ, Blaauw M, Plunkett G. 2012. Ecohydrological feedbacks confound peat-based climate reconstructions. *Geophys Res Lett.* <https://doi.org/10.1029/2012GL051500>.
- Swindles GT, Morris PJ, Mullan DJ, Payne RJ, Roland TP, Amesbury MJ, Lamentowicz M, Turner TE, Gallego-Sala A, Sim T, and others 2019. Widespread drying of european peatlands in recent centuries. *Nature Geoscience* 12(11):922–928. <https://doi.org/10.1038/s41561-019-0462-z>.
- Tahvanainen T. 2011. Abrupt ombrotrophication of a boreal aapa mire triggered by hydrological disturbance in the catchment. *J Ecol* 99(2):404–415. <https://doi.org/10.1111/j.1365-2745.2010.01778.x>.
- Tahvanainen T, Sallantausta T, Heikkilä R, Tolonen K. 2002. Spatial variation of mire surface water chemistry and vegetation in northeastern finland. *Ann Bot Fenn* 39(3):235–251.
- Ter Braak CJF, Barendregt LG. 1986. Weighted averaging of species indicator values: Its efficiency in environmental calibration. *Math Biosci* 78(1):57–72. [https://doi.org/10.1016/0025-5564\(86\)90031-3](https://doi.org/10.1016/0025-5564(86)90031-3).
- Tolonen K. 1967. Pohjois-karjalan metsien, soiden ja järvien kehityksestä. on the development of forests, mires and lakes in northern karelia, finland. *Mires and Peat* 17:1–6.
- Treat CC, Bloom AA, Marushchak ME. 2018. Nongrowing season methane emissions—a significant component of annual emissions across northern ecosystems. *Glob Change Biol* 24(8):3331–3343. <https://doi.org/10.1111/gcb.14137>.
- Tsyganov AN, Kupriyanov DA, Babeshko KV, Borisova TV, Chernyshov VA, Volkova EM, Chekova DA, Mazei YA, Novenko EY. 2019. Autogenic and allogenic factors affecting development of a floating sphagnum-dominated peat mat in a karst pond basin. *The Holocene* 29(1):120–129. <https://doi.org/10.1177/0959683618804631>.
- Väliranta M, Salojärvi N, Vuorsalo A, Juutinen S, Korhola A, Luoto M, Tuittila E. 2017. Holocene fen–bog transitions, current status in finland and future perspectives. *The Holocene* 27(5):752–764. <https://doi.org/10.1177/0959683616670471>.
- Väliranta M, Oinonen M, Seppä H, Korkonen S, Juutinen S, Tuittila E. 2014. Unexpected problems in AMS 14C dating of fen peat. *Radiocarbon* 56(1):95–108. <https://doi.org/10.2458/56.16917>.
- Voigt C, Marushchak ME, Lamprecht RE, Jackowicz-Korczyński M, Lindgren A, Mastepanov M, Granlund L, Christensen TR, Tahvanainen T, Martikainen PJ, and others 2017. Increased nitrous oxide emissions from arctic peatlands after permafrost thaw. *Proc Natl Acad Sci* 114(24):6238–6243. <https://doi.org/10.1073/pnas.1702902114>.
- Walther G, Post E, Convey P, Menzel A, Parmesan C, Beebee TJC, Fromentin J, Hoegh-Guldberg O, Bairlein F. 2002. Ecological responses to recent climate change. *Nature* 416(6879):389–395. <https://doi.org/10.1038/416389a>.
- Young DM, Baird AJ, Gallego-Sala A, Loisel J. 2021. A cautionary tale about using the apparent carbon accumulation rate (aCAR) obtained from peat cores. *Scientific Reports* 11(1):9547. <https://doi.org/10.1038/s41598-021-88766-8>
- Zhang H, Tuittila E, Korrensalo A, Laine AM, Uljas S, Welti N, Kerttula J, Maljanen M, Elliott D, Vesala T, and others. 2021. Methane production and oxidation potentials along a fen-bog gradient from southern boreal to subarctic peatlands in finland. *Glob Change Biol* 227:4449–4464. <https://doi.org/10.1111/gcb.15740>.